Nonadiabatic couplings and nonadiabatic dynamics within TDDFT

Ivano Tavernelli

EPFL, LCBC, Lausanne (Switzerland)

CECAM workshop Nov. 6-9 2012
Lausanne, Switzerland

November 6, 2012

Nonadiabatic effects requires quantum nuclear dynamics

The nuclear dynamics cannot be described by a single classical trajectory (like in the ground state -adiabatically separated- case)

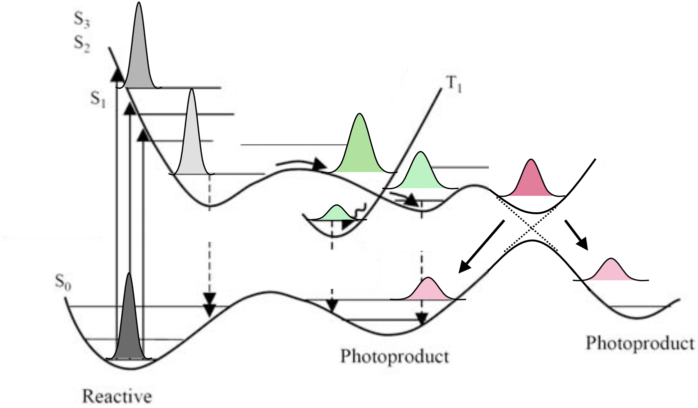

Nonadiabatic dynamics: Multi-trajectory solutions

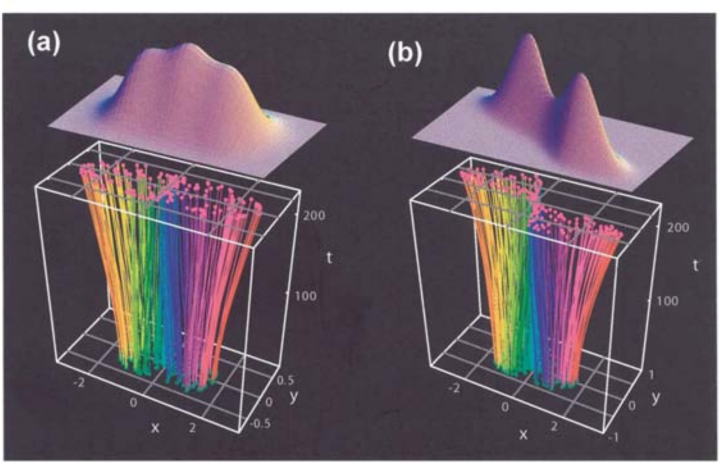

Starting point

The starting point is the molecular time-dependent Schrödinger equation:

$$\hat{H}\Psi(\boldsymbol{r},\boldsymbol{R},t) = i\hbar\frac{\partial}{\partial t}\Psi(\boldsymbol{r},\boldsymbol{R},t)$$

where $\hat{H}$ is the molecular time-independent Hamiltonian and $\Psi(\boldsymbol{r},\boldsymbol{R},t)$ the total wavefunction (nuclear + electronic) of our system.

Solutions of the coupled electron-nuclear dynamics can be derived using different Ansätze for the total molecular wavefunction $\Psi(\boldsymbol{r},\boldsymbol{R},t)$

Ansätze

$$\Psi(\boldsymbol{r},\boldsymbol{R},t) \xrightarrow[\text{Huang}]{\text{Born-}} \sum_{j}^{\infty}\Phi_j(\boldsymbol{r};\boldsymbol{R})\Omega_j(\boldsymbol{R},t)$$

$$\Psi(\boldsymbol{r},\boldsymbol{R},t) \xrightarrow{\text{Ehrenfest}} \Phi(\boldsymbol{r};\boldsymbol{R},t)\Omega(\boldsymbol{R},t)\exp\left[\frac{i}{\hbar}\int_{t_0}^{t}E_{el}(t')dt'\right]$$

$$\Psi(\boldsymbol{r},\boldsymbol{R},t) \xrightarrow[\text{factor.}]{\text{Exact-}} \Phi(\boldsymbol{r},t)\Omega(\boldsymbol{R},t)$$

On-the-fly nonadiabatic dynamics with trajectories

a. Potential energy surfaces

Computed on-the-fly using linear response TDDFT

b. Propagation of the nuclear wavepacket

The wavepacket dynamics is replaced by the time-propagation of a swarm of trajectories. We consider two options:

- Classical trajectories driven by forces computed as gradient of the TDDFT PESs
- Quantum (Bohmian) trajectories driven by classical and quantum potentials both computed within TDDFT

c. Nonadiabatic couplings between the PESs

Transition between PESs governed by the nonadiabatic couplings derived from TDDFT

d. Coupling with the environment

Coupling with external (static and time-dependent) fields at TDDFT level

On-the-fly nonadiabatic dynamics with trajectories

a. Potential energy surfaces

Computed on-the-fly using linear response TDDFT

b. Propagation of the nuclear wavepacket

The wavepacket dynamics is replaced by the time-propagation of a swarm of trajectories. We consider two options:

- Classical trajectories driven by forces computed as gradient of the TDDFT PESs
- Quantum (Bohmian) trajectories driven by classical and quantum potentials both computed within TDDFT

c. Nonadiabatic couplings between the PESs

Transition between PESs governed by the nonadiabatic couplings derived from TDDFT

d. Coupling with the environment

Coupling with external (static and time-dependent) fields at TDDFT level

On-the-fly nonadiabatic dynamics with trajectories

a. Potential energy surfaces

Computed on-the-fly using linear response TDDFT

b. Propagation of the nuclear wavepacket

The wavepacket dynamics is replaced by the time-propagation of a swarm of trajectories. We consider two options:

- Classical trajectories driven by forces computed as gradient of the TDDFT PESs
- Quantum (Bohmian) trajectories driven by classical and quantum potentials both computed within TDDFT

c. Nonadiabatic couplings between the PESs

Transition between PESs governed by the nonadiabatic couplings derived from TDDFT

d. Coupling with the environment

Coupling with external (static and time-dependent) fields at TDDFT level

On-the-fly nonadiabatic dynamics with trajectories

a. Potential energy surfaces

Computed on-the-fly using linear response TDDFT

b. Propagation of the nuclear wavepacket

The wavepacket dynamics is replaced by the time-propagation of a swarm of trajectories. We consider two options:

- Classical trajectories driven by forces computed as gradient of the TDDFT PESs
- Quantum (Bohmian) trajectories driven by classical and quantum potentials both computed within TDDFT

c. Nonadiabatic couplings between the PESs

Transition between PESs governed by the nonadiabatic couplings derived from TDDFT

d. Coupling with the environment

Coupling with external (static and time-dependent) fields at TDDFT level

On-the-fly nonadiabatic dynamics with trajectories

a. Potential energy surfaces

Computed on-the-fly using linear response TDDFT

b. Propagation of the nuclear wavepacket

The wavepacket dynamics is replaced by the time-propagation of a swarm of trajectories. We consider two options:

- Classical trajectories driven by forces computed as gradient of the TDDFT PESs
- Quantum (Bohmian) trajectories driven by classical and quantum potentials both computed within TDDFT

c. Nonadiabatic couplings between the PESs

Transition between PESs governed by the nonadiabatic couplings derived from TDDFT

d. Coupling with the environment

Coupling with external (static and time-dependent) fields at TDDFT level

On-the-fly nonadiabatic dynamics with trajectories

a. Potential energy surfaces

Computed on-the-fly using linear response TDDFT

b. Propagation of the nuclear wavepacket

The wavepacket dynamics is replaced by the time-propagation of a swarm of trajectories. We consider two options:

- Classical trajectories driven by forces computed as gradient of the TDDFT PESs
- Quantum (Bohmian) trajectories driven by classical and quantum potentials both computed within TDDFT

c. Nonadiabatic couplings between the PESs

Transition between PESs governed by the nonadiabatic couplings derived from TDDFT

d. Coupling with the environment

Coupling with external (static and time-dependent) fields at TDDFT level

On-the-fly nonadiabatic dynamics with trajectories

a. Potential energy surfaces

Computed on-the-fly using linear response TDDFT

b. Propagation of the nuclear wavepacket

The wavepacket dynamics is replaced by the time-propagation of a swarm of trajectories. We consider two options:

- Classical trajectories driven by forces computed as gradient of the TDDFT PESs
- Quantum (Bohmian) trajectories driven by classical and quantum potentials both computed within TDDFT

c. Nonadiabatic couplings between the PESs

Transition between PESs governed by the nonadiabatic couplings derived from TDDFT

d. Coupling with the environment

Coupling with external (static and time-dependent) fields at TDDFT level

On-the-fly nonadiabatic dynamics with trajectories

a. Potential energy surfaces

Computed on-the-fly using linear response TDDFT

b. Propagation of the nuclear wavepacket

The wavepacket dynamics is replaced by the time-propagation of a swarm of trajectories. We consider two options:

- Classical trajectories driven by forces computed as gradient of the TDDFT PESs
- Quantum (Bohmian) trajectories driven by classical and quantum potentials both computed within TDDFT

c. Nonadiabatic couplings between the PESs

Transition between PESs governed by the nonadiabatic couplings derived from TDDFT

d. Coupling with the environment

Coupling with external (static and time-dependent) fields at TDDFT level

On-the-fly nonadiabatic dynamics with trajectories

a. Potential energy surfaces

Computed on-the-fly using linear response TDDFT

b. Propagation of the nuclear wavepacket

The wavepacket dynamics is replaced by the time-propagation of a swarm of trajectories. We consider two options:

- Classical trajectories driven by forces computed as gradient of the TDDFT PESs
- Quantum (Bohmian) trajectories driven by classical and quantum potentials both computed within TDDFT

c. Nonadiabatic couplings between the PESs

Transition between PESs governed by the nonadiabatic couplings derived from TDDFT

d. Coupling with the environment

Coupling with external (static and time-dependent) fields at TDDFT level

LR-TDDFT - Energies and forces

- Using the linear response orbitals (perturbative solution: Sternheimer 1951)

$$\sum_{j=1}^{N}(H_0^\sigma\,\delta_{ij}-\epsilon_{ij})|\phi'_{I,j\sigma}\rangle+\mathcal{Q}^\sigma\,\delta v_I^{\sigma\,\mathrm{SCF}}|\phi_{i\sigma}\rangle=\omega_I|\phi'_{I,i\sigma}\rangle$$

- Using the virtual Kohn-Sham orbital expansion (Casida formulation)

$$\begin{bmatrix}\mathcal{A}(\omega) & \mathcal{B}(\omega)\\ \mathcal{B}(\omega) & \mathcal{A}(\omega)\end{bmatrix}\begin{bmatrix}\mathbf{x}_I\\ \mathbf{y}_I\end{bmatrix}=\omega_I\begin{bmatrix}\mathcal{C} & 0\\ 0 & -\mathcal{C}\end{bmatrix}\begin{bmatrix}\mathbf{x}_I\\ \mathbf{y}_I\end{bmatrix}$$

- Analytic excited state forces (using the Lagrange multiplier formalism)

$$\frac{dE_{tot}[c^{\{0\}},x,y]}{d\eta}=\frac{dE_{KS}[c^{\{0\}}]}{d\eta}+\frac{d\omega[c^{\{0\}},x,y]}{d\eta}$$

[J. Hutter, JCP, 118, 3928 (2003)]

- Solution always within the adiabatic approximation (no memory kernel)

Trajectory based solution of the nuclear dynamics

In trajectory based solutions of the quantum dynamics we obtain a Newton-like equation of motion for the nuclei

$$M_\beta \frac{d^2 R_\beta}{(dt^J)^2} = -\nabla_\beta \left[E^J_{el}(R) + \mathcal{Q}_J(R,t) + \mathcal{D}_{JI}(R,t) \right]$$

$\mathcal{Q}_J(R,t)$: adiabatic quantum potential

$\mathcal{D}_{JI}(R,t)$: nonadiabatic couplings

1. NonAdiabatic Ehrenfest Dynamics (mean-field one-trajectory solution)
2. NonAdiabatic Bohmian Dynamics (NABDY) provides an exact solution for the two extra terms: $\mathcal{Q}$ and $\mathcal{D}_{JI}$. [PCCP, 13, 3231 (2011)]
3. Trajectory Surface Hopping Dynamics (TSH) is derived from the so called Independent Trajectory Approximation (ITA) together with [Tully, JCP, 1971]
    - $\hbar \to 0$ for the action (classical trajectories: $\mathcal{Q} = 0$)
    - stochastic (*phenomenological*) description of the couplings $\mathcal{D}_{JI}$: trajectory surface hopping algorithm.

Trajectory based solution of the nuclear dynamics

In trajectory based solutions of the quantum dynamics we obtain a Newton-like equation of motion for the nuclei

$$M_\beta \frac{d^2 R_\beta}{(dt^J)^2} = -\nabla_\beta \left[E_{el}^J(R) + \mathcal{Q}_J(R,t) + \mathcal{D}_{JI}(R,t) \right]$$

$\mathcal{Q}_J(R,t)$: adiabatic quantum potential

$\mathcal{D}_{JI}(R,t)$: nonadiabatic couplings

1. NonAdiabatic Ehrenfest Dynamics (mean-field one-trajectory solution)
2. NonAdiabatic Bohmian Dynamics (NABDY) provides an exact solution for the two extra terms: $\mathcal{Q}$ and $\mathcal{D}_{JI}$. [PCCP, 13, 3231 (2011)]
3. Trajectory Surface Hopping Dynamics (TSH) is derived from the so called Independent Trajectory Approximation (ITA) together with [Tully, JCP, 1971]
    - $\hbar \rightarrow 0$ for the action (classical trajectories: $\mathcal{Q} = 0$)
    - stochastic (*phenomenological*) description of the couplings $\mathcal{D}_{JI}$: trajectory surface hopping algorithm.

TSH nonadiabatic MD ($\hbar \to 0$ for $\Omega_l(\boldsymbol{R}, t)$ and more)

There is no derivation of TSH dynamics. The fundamental hypothesis beyond TSH is that it is possible to design a dynamics that consists of:

- classical (*adiabatic*) time evolution of the nuclear trajectories on adiabatic states solution of the Schrödinger equation for the electronic sub-system
- propagation of a "quantum" amplitude, $C_k^\alpha(t)$, associated to each PES, k

$$\Psi^\alpha(\boldsymbol{r}, \boldsymbol{R}, t) = \sum_k^\infty C_k^\alpha(t)\Phi_k(\boldsymbol{r}; \boldsymbol{R})$$

  (the label α is to recall that we have a different contribution from each different trajectory.)

- transitions (hops) of the trajectories between electronic states according to a stochastic algorithm, which depends on the nonadiabatic couplings and the amplitudes $C_k^\alpha(t)$ ($\leftarrow$ need of el.-ph. couplings).

See: J. Tully, *Faraday discussion*, **110**, 407 (1998)

TSH nonadiabatic MD ($\hbar \to 0$ for $\Omega_l(\boldsymbol{R}, t)$ and more)

The main claim of TSH is that, the collection of a large enough set of independent trajectories gives an accurate representation of the nuclear wave packet

$$\rho_k^{CL}(\boldsymbol{R}^\alpha, t^\alpha) = \frac{N_k^\alpha(\boldsymbol{R}^\alpha, dV, t^\alpha)}{N_{tot}} \frac{1}{dV} \sim |\Omega_k(\boldsymbol{R}^\alpha, t^\alpha)|^2 \sim |C_{k,\boldsymbol{R}^\alpha,t^\alpha}^\alpha|^2$$

Inserting

$$\Psi^\alpha(\boldsymbol{r}, \boldsymbol{R}, t) = \sum_k^\infty C_k^\alpha(t) \Phi_k(\boldsymbol{r}; \boldsymbol{R})$$

into the time-dependent Schrödinger equation for the electrons and after some rearrangement, we obtain:

$$i\hbar \dot{C}_k^\alpha(t) = \sum_j C_j^\alpha(t)(H_{kj} - i\hbar \dot{\boldsymbol{R}}^\alpha \cdot \boldsymbol{d}_{kj}^\alpha)$$

with $H_{kj} = \langle \Phi_k(\boldsymbol{r}; \boldsymbol{R}) | \hat{\mathcal{H}}_{el} | \Phi_j(\boldsymbol{r}; \boldsymbol{R}) \rangle$ ← densityfunctionalization of TSH.
In the adiabatic representation, we have $H_{kk} = E_k^{el}$ and $H_{kj} = 0$.

On-the-fly TDDFT/TSH: photo-excited $CH_2NH_2^+$

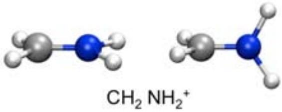

Protonated formaldimine as a model compound for the study of the isomerization of retinal.

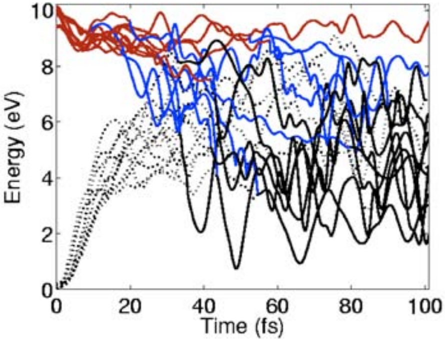

Photo-excitation promotes the system mainly into S_2.

Relaxation involves at least 3 states:
S_0 (GS), S_1 and S_2.

[E. Tapavicza, I. T., U. Rothlisberger, PRL, **98**, 023001 (2007)]

The quest for matrix elements $\langle\Phi|\mathcal{O}|\Psi\rangle$ in TDDFT

TDDFT energies and forces are available since a decade, but in order to perform nonadiabatic dynamics (TSH or Bohmian) one needs to express nonadiabatic coupling elements (NAC) and nonadiabatic coupling vectors (NACV)

$$d_{J0}^{\gamma}[\Phi_0, \Phi_J] = \frac{\langle\Phi_0|\nabla\mathcal{H}|\Phi_J\rangle}{\Delta E_{J0}}$$

$$d_{J0}^{\gamma}[\rho, \delta\rho] = ?$$

as a functional of the electronic density $\rho(r)$ or, equivalently, of the occupied Kohn-Sham orbitals $\{\phi_i(r)\}$.

Additional care is required for the case of matrix elements between pairs of excited states, which calculation goes beyond simple linear response theory

$$o_{JI}^{\gamma}(\tau) = \langle\Phi_I|\mathcal{O}|\Phi_J\rangle \, .$$

Auxiliary wavefunctions for LR-TDDFT

It is possible to descrobe linear response quantities within TDDFT using a set of auxiliary many-electron wavefunctions.

- I.T., E. Tapavicza, U. Rothlisberger, JCP, **130**, 124107 (2007)
- I.T., B. F. E. Curchod, U. Rothlisberger, JCP, **131**, 196101 (2009)
- I.T., B. F. E. Curchod, A. Laktionov, U. Rothlisberger, JCP, **133**, 194104 (2010)

They are given as a linear combination of singly excited Slater determinants

The auxiliary many-electron wavefunctions (AX WF)

$$\tilde{\psi}_I[\{\phi.\}] = \sum_{ia\sigma} c^I_{ia\sigma}\, \hat{a}^\dagger_{a\sigma} \hat{a}_{i\sigma} \tilde{\psi}_0[\{\phi.\}]$$

with

$$c^I_{ia\sigma} \equiv \sqrt{\frac{S^{-1}_{ia\sigma}}{\omega_{0I}}}\, e^I_{ia\sigma}$$

where $\tilde{\psi}_0[\{\phi.\}]$ is the Slater determinant of all occupied KS orbitals $\{\phi_{i\sigma}\}_{i=1}^N$, and $\hat{a}^\dagger_{a\sigma}$, $\hat{a}_{i\sigma}$ are the creation (of virtual orbitals, $\phi_{a\sigma}$) and annihilation operators.

Derivation: The density response SOS formula

In TDDFT the density response $\chi(\omega)$ is

$$\chi(\omega) = \mathbb{S}^{-1/2}(\omega^2\mathbb{I} - \Omega(\omega))^{-1}\mathbb{S}^{-1/2}$$

Using the TDDFT eigenvectors, $\mathbf{Z}_n$, of the pseudoeigenvalue equation,

$$\mathbf{\Omega}\mathbf{Z}_n = \omega_{0n}^2\mathbf{Z}_n\,,$$

the spectral representation of $(\omega^2\mathbb{I} - \Omega(\omega))^{-1}$ becomes

$$(\omega^2\mathbb{I} - \Omega(\omega))^{-1} = \sum_n \frac{\boldsymbol{Z}_n\boldsymbol{Z}_n^\dagger}{\omega_n^2 - \omega^2}$$

Therefore

$$\chi(\omega) = \sum_n \frac{\mathbb{S}^{-1/2}\boldsymbol{Z}_n\boldsymbol{Z}_n^\dagger\mathbb{S}^{-1/2}}{\omega_n^2 - \omega^2}$$

and finally the perturbation of any observable ($\delta\mathcal{O}(\omega) = \sum_{ij\sigma} o_{ij\sigma}\delta P_{ij\sigma}$)

$$\delta\mathcal{O}^{TDDFT}(\omega) = \sum_n \sum_{ij\sigma,kl\tau} o_{ij\sigma}\frac{(\mathbb{S}^{-1/2}\boldsymbol{Z}_n)_{ik\sigma}(\boldsymbol{Z}_n^\dagger\mathbb{S}^{-1/2})_{kl\tau}}{\omega_n^2 - \omega^2}v'_{kl\tau}E(\omega)\,.$$

From standard MBPT

$$\delta\mathcal{O}^{MBPT}(\omega)=\sum_n \frac{2\omega_{i0}\langle\Psi_0|\hat{\mathcal{O}}|\Psi_n\rangle\langle\Psi_n|\hat{v}'E(\omega)|\Psi_0\rangle}{\omega_{n0}^2-\omega^2}$$

Equating $\delta\mathcal{O}^{TDDFT}(\omega)$ with $\delta\mathcal{O}^{MBPT}(\omega)$ residue-by-residue, one gets

$$\langle\Psi_0|\hat{\mathcal{O}}|\Psi_n\rangle=\sum_{ij\sigma}^{(f_{i\sigma}-f_{j\sigma})>0}\frac{1}{\sqrt{\omega_n}}o_{ij\sigma}(\mathbb{S}^{-1/2}\boldsymbol{Z}_n)_{ij\sigma}$$

For any one-body operator, $\hat{\mathcal{O}}$, this mapping between MBPT and TDDFT gives

$$\mathbf{O}^{\dagger}\mathbb{S}^{-1/2}\mathbf{Z}_n=\omega_{0n}^{1/2}\langle\Psi_0|\hat{\mathcal{O}}|\Psi_n\rangle$$

where the operator $\hat{\mathcal{O}}=\sum_{ia\sigma}o_{ia\sigma}\hat{a}^{\dagger}_{i\sigma}\hat{a}_{a\sigma}$ has components $o_{ia\sigma}=\langle\phi_{i\sigma}|\hat{\mathcal{O}}|\psi_{a\sigma}\rangle$ [1] with $\omega_{0n}=E_n-E_0$. All matrices and vectors are given in the basis of KS orbitals $\{\phi_{i\sigma}\}$ with corresponding occupations $f_{i\sigma}$ and orbital energies $\epsilon_{i\sigma}$.

---

[1] $\sum_{ia\sigma}$ stands for $\sum_{i=1}^{N}\sum_{a=1}^{\infty}\sum_{\sigma\in\{\alpha,\beta\}}$.

Applications of the AX WF

- The *nonadiabatic coupling elements* at the mid step $t + \delta t/2$ of a TDDFT MD dynamics can therefore be calculated as

$$\dot{\boldsymbol{R}} \cdot \boldsymbol{d}_{\mathbf{0}\boldsymbol{I}}|_{\boldsymbol{t}+\delta \boldsymbol{t}/\mathbf{2}}[\{\phi.\}] = \left\langle \tilde{\psi}_{\mathbf{0}}(\boldsymbol{r};\boldsymbol{R}(t)) \middle| \nabla_{\boldsymbol{R}} \middle| \tilde{\psi}_{\boldsymbol{I}}(\boldsymbol{r};\boldsymbol{R}(t)) \right\rangle \cdot \dot{\boldsymbol{R}} = \left\langle \tilde{\psi}_{\mathbf{0}}(\boldsymbol{r};\boldsymbol{R}(t)) \middle| \frac{\partial}{\partial t} \middle| \tilde{\psi}_{\boldsymbol{I}}(\mathbf{r};\boldsymbol{R}(t)) \right\rangle$$

$$\simeq \frac{1}{2\delta t}\left[\langle \tilde{\psi}_{\mathbf{0}}(\boldsymbol{r};\boldsymbol{R}(t)) | \tilde{\psi}_{\boldsymbol{I}}(\boldsymbol{r};\boldsymbol{R}(t+\delta t))\rangle - \langle \tilde{\psi}_{\mathbf{0}}(\boldsymbol{r};\boldsymbol{R}(t+\delta t)) | \tilde{\psi}_{\boldsymbol{I}}(\boldsymbol{r};\boldsymbol{R}(t))\rangle\right]$$

- The *nonadiabatic coupling vectors*

$$\mathbf{d}_{0I}[\{\phi.\}] = \langle \tilde{\psi}_0(\mathbf{R}) | \nabla_{\mathbf{R}} | \tilde{\psi}_I(\mathbf{R}) \rangle = \frac{\langle \tilde{\psi}_0(\boldsymbol{R}) | \nabla_{\boldsymbol{R}} \mathcal{H} | \tilde{\psi}_I(\boldsymbol{R}) \rangle}{E_I(\boldsymbol{R}) - E_0(\boldsymbol{R})}$$

- The *transition dipole matrix elements*

$$\boldsymbol{\mu}_{0I}[\{\phi.\}] = \langle \tilde{\psi}_0(\mathbf{R}) | \hat{\mu} | \tilde{\psi}_I(\mathbf{R}) \rangle = -e\omega_{0I}^{-1/2} \boldsymbol{r}^{\dagger} \mathbf{S}^{-1/2} \mathbf{e}_I$$

- The Spin-Orbit Couplings (Breit-Pauli Hamiltonian)

$$\boldsymbol{S}_{0I}[\{\phi.\}] = \langle \tilde{\psi}_0(\mathbf{R}) | \frac{Z}{2m_e^2 c^2 r^3} \boldsymbol{s} \cdot \boldsymbol{l} | \tilde{\psi}_I(\mathbf{R}) \rangle$$

Matrix elements for pairs of excited states

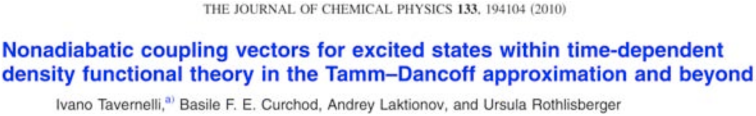

THE JOURNAL OF CHEMICAL PHYSICS **133**, 194104 (2010)

Nonadiabatic coupling vectors for excited states within time-dependent density functional theory in the Tamm–Dancoff approximation and beyond

Ivano Tavernelli,[a] Basile F. E. Curchod, Andrey Laktionov, and Ursula Rothlisberger

The equations for the NACVs are obtained from the one-to-one (or residue-by-residue) mapping between

- $\beta^{(\alpha\beta\gamma)}_{MBPT}(\omega_1,\omega_2)[\Psi_0,\Psi_1,\Psi_2]$: MBPT second-order polarizability
- $\beta^{(\alpha\beta\gamma)}_{TDDFT}(\omega_1,\omega_2)[\rho,\delta\rho]$: TDDFT second-order polarizability.
  (SOS representation of $\beta^{(\alpha\beta\gamma)}_{TDDFT}$ through **bosonization** (HA) of the KS excitation operators).

The same procedure used in the derivation of the matrix elements between ground and excited states can be followed for the calculation of the second order response matrix elements $\langle\Psi_I|\hat{O}|\Psi_J\rangle$, where both states Ψ_I and Ψ_J are linear response excited states.

MBPT second-order polarizability

Within the many-body formulation of quantum mechanics in second quantization, the SOS second-order density-density response function is obtained using a perturbative approach applied to the molecular Hamiltonian and reads [2]

$$\beta^{(\alpha\beta\gamma)}_{MBPT}(\omega_1,\omega_2) = \frac{1}{2}\sum_{IJ=1}^{M}\sum_{\mathrm{perm}(\omega_1,\omega_2)}\left[\frac{\mu^{(\alpha)}_{J}\mu^{(\beta)}_{-JI}\mu^{(\gamma)}_{-I}}{(\Omega_J-\omega_1-\omega_2)(\Omega_I-\omega_1)}+\frac{\mu^{(\alpha)}_{J}\mu^{(\beta)}_{-JI}\mu^{(\gamma)}_{-I}}{(\Omega_J+\omega_2)(\Omega_I+\omega_1+\omega_2)}+\frac{\mu^{(\alpha)}_{JI}\mu^{(\beta)}_{-J}\mu^{(\gamma)}_{-I}}{(\Omega_J+\omega_2)(\Omega_I-\omega_1)}\right]$$

with $\mu^{(\alpha)}_{J}=\langle\Psi_0|\mu^{(\alpha)}|\Psi_J\rangle$ and $\mu^{(\alpha)}_{-JI}=\langle\Psi_J|\mu^{(\alpha)}|\Psi_I\rangle$.

---

[2] J. F. Ward, *Rev. Mod. Phys.* **37**, 1 (1965); B. J. Orr, J. F. Ward, *Mol. Phys.* **20**, 513 (1971).

TDDFT second-order polarizability

The second-order TDDFT density response functions are given by [3]

$$\beta^{(2)}(\omega_1,\omega_2,\mathbf{r},\mathbf{r}',\mathbf{r}'') = \sum_{IJK} \frac{V''_{-IJK}\mu_I(\mathbf{r})\mu_{-J}(\mathbf{r}')\mu_{-K}(\mathbf{r}'')s_I s_J s_K}{(\Omega_I-\omega_1-\omega_2)(\Omega_J-\omega_1)(\Omega_K-\omega_2)} - \frac{1}{2}\sum_{IJ}\frac{\mu_{-IJ}(\mathbf{r})\mu_I(\mathbf{r}')\mu_{-J}(\mathbf{r}'')s_I s_J}{(\Omega_I-\omega_1-\omega_2)(\Omega_J-\omega_1)}$$
$$- \frac{1}{2}\sum_{IJ}\frac{\mu_{-IJ}(\mathbf{r})\mu_I(\mathbf{r}')\mu_{-J}(\mathbf{r}'')s_I s_J}{(\Omega_I-\omega_1-\omega_2)(\Omega_J-\omega_2)} - \frac{1}{2}\sum_{IJ}\frac{\mu_{IJ}(\mathbf{r})\mu_{-I}(\mathbf{r}')\mu_{-J}(\mathbf{r}'')s_I s_J}{(\Omega_I-\omega_1)(\Omega_J-\omega_2)}$$

where

- $s_I = \mathrm{sign}(I)$,
- $I, J, K = \pm 1, \pm 2, \ldots,$
- V''_{IJK} are the second-order coupling terms between excited states
- ξ_I are the eigenvectors of the LR-TDDFT eigenvalue equations

$$\mathcal{L}\,\xi_I = \Omega_I \xi_I\,.$$

---

[3] S. Tretiak and S. Mukamel, *Chem. Rev.*, **102**, 3171 (2002); S. Tretiak and V. Chernyak, *J Chem Phys*, **119**, 8809 (2003); I. T, B.F.E. Curchod, A. Laktionov, and U. Rothlisberger, *J. Chem. Phys.*, **133**, 194104 (2010)..

TDDFT second-order polarizability

Required quantities: [4]

$$\begin{aligned} V''_{IJK} =& \frac{1}{2} Tr\big[(I-2\rho_0)\big((\xi_J\xi_K+\xi_K\xi_J)V''(\xi_I)+ \\ & +(\xi_I\xi_J+\xi_J\xi_I)V''(\xi_K)+(\xi_I\xi_K+\xi_K\xi_I)V''(\xi_J)\big)\big] \end{aligned}$$

with

$$\begin{aligned} V''(\xi_I)(\boldsymbol{r})\xi_J &= V'[\xi_I](\boldsymbol{r})\xi_J + V''_{nl}[\xi_I,\xi_J](\boldsymbol{r})\rho_0(\boldsymbol{r}) \\ V'[\xi_I](\boldsymbol{r}) &= \int d\boldsymbol{r}'\, f_{xc}[\rho](\boldsymbol{r},\boldsymbol{r}')\xi_I(\boldsymbol{r}') \\ V''_{nl}[\xi_I,\xi_J](\boldsymbol{r}) &= \int d\boldsymbol{r}' \int d\boldsymbol{r}''\, g_{xc}[\rho](\boldsymbol{r},\boldsymbol{r}',\boldsymbol{r}'')\xi_I(\boldsymbol{r}')\xi_J(\boldsymbol{r}'') \end{aligned}$$

and

$$\rho_{I,JK}(\boldsymbol{r}) = -\xi_I(\xi_J\xi_K+\xi_K\xi_J)(\boldsymbol{r})\,.$$

---

[4] S. Tretiak and S. Mukamel, *Chem. Rev.*, **102**, 3171 (2002); S. Tretiak and V. Chernyak, *J Chem Phys*, **119**, 8809 (2003); I. T, B.F.E. Curchod, A. Laktionov, and U. Rothlisberger, *J. Chem. Phys.*, **133**, 194104 (2010)..

TDDFT second-order polarizability

Using the following definition of the dipole matrices

$$\boldsymbol{\mu}_I = Tr([\rho_0, \xi_I][\mu, \rho_0])$$
$$\boldsymbol{\mu}_{IJ} = Tr([\rho_0, \xi_I][\mu, \xi_J])$$

the second-order polarizability within TDDFT becomes

$$\beta^{(\alpha\beta\gamma)}(\omega_1, \omega_2) = -\sum_{IJK=-M}^{M} \frac{V''_{-IJK}\,\mu_I^{(\alpha)}\mu_{-J}^{(\beta)}\mu_{-K}^{(\gamma)} s_I s_J s_K}{(\Omega_I - \omega_1 - \omega_2)(\Omega_J - \omega_1)(\Omega_K - \omega_2)} + \frac{1}{2}\sum_{IJ=-M}^{M} \frac{\mu_{-IJ}^{(\beta)}\mu_I^{(\alpha)}\mu_{-J}^{(\gamma)} s_I s_J}{(\Omega_I - \omega_1 - \omega_2)(\Omega_J - \omega_1)}$$
$$+ \frac{1}{2}\sum_{IJ=-M}^{M} \frac{\mu_{-IJ}^{(\beta)}\mu_I^{(\alpha)}\mu_{-J}^{(\gamma)} s_I s_J}{(\Omega_I - \omega_1 - \omega_2)(\Omega_J - \omega_2)} + \frac{1}{2}\sum_{IJ=-M}^{M} \frac{\mu_{IJ}^{(\alpha)}\mu_{-I}^{(\beta)}\mu_{-J}^{(\gamma)} s_I s_J}{(\Omega_I - \omega_1)(\Omega_J - \omega_2)}$$

where $\alpha, \beta, \gamma \in \{x, y, z\}$, and $\boldsymbol{\mu}_{-IJ}$ is the transition dipole between states I and J for which $\boldsymbol{\mu}_I = \boldsymbol{\mu}^*_{-I}$ and $\boldsymbol{\mu}_{-IJ} = \boldsymbol{\mu}^*_{-JI}$

However, this is NOT a SOS formula (coupling terms V''_{-IJK}).

Bosonization of the TDDFT second order response

Mukamel, Tretiak, Chernyak and Berman propose a classical system of coupled harmonic oscillators (bosons) that shares the same linear and second-order response properties of TDDFT.

$$\sum_\sigma \hat{c}^\dagger_{r\sigma}\hat{c}_{s\sigma} \longrightarrow \sum_\sigma \tilde{c}^\dagger_{r\sigma}\tilde{c}_{s\sigma}$$

Comparing term-by-term β^{SOS}_{MBPT} with $\beta^{(B)\,SOS}_{TDDFT}$

$$\langle\Psi_0|\sum_\sigma \hat{c}^\dagger_{r\sigma}\hat{c}_{s\sigma}|\Psi_0\rangle = (\rho_0)_{rs}$$

$$\langle\Psi_0|\sum_\sigma \hat{c}^\dagger_{r\sigma}\hat{c}_{s\sigma}|\Psi^{(1)}_I\rangle = (\xi_I)_{rs}$$

$$\langle\Psi_0|\sum_\sigma \hat{c}^\dagger_{r\sigma}\hat{c}_{s\sigma}|\Psi^{(2)}_{IJ}\rangle = \frac{1}{\sqrt{1+\delta_{IJ}}}\Big[([[\xi_I,\rho_0],\xi_J])_{rs} + \sum_{K>0}\Big(\frac{V''_{IJ-K}(\xi_K)_{rs}}{\Omega_I+\Omega_J-\Omega_K} - \frac{V''_{IJK}(\xi^\dagger_K)_{rs}}{\Omega_I+\Omega_J+\Omega_K}\Big)\Big]$$

$$\langle\Psi^{(1)}_I|\sum_\sigma \hat{c}^\dagger_{r\sigma}\hat{c}_{s\sigma}|\Psi^{(1)}_J\rangle = (\rho_0)_{rs}\delta_{IJ} + ([[\xi^\dagger_I,\rho_0],\xi_J])_{rs} + \sum_{K>0}\frac{V''_{-IJ-K}(\xi_K)_{rs}}{\Omega_J-\Omega_I-\Omega_K} - \frac{V''_{I-J-K}(\xi^\dagger_K)_{rs}}{\Omega_J-\Omega_I+\Omega_K})$$

where $\xi^\dagger_I = \xi_{-I}$.

The auxiliary many-electron wavefunction approach

Considering only terms up to second order in $\boldsymbol{Z}_I$ where $(\boldsymbol{Z}_I \sim \boldsymbol{X}_I + \boldsymbol{Y}_I)$ we compare results for $\langle \Psi_J | \hat{O} | \Psi_I \rangle$ obtained using the "bosonization" (B) and the "auxiliary wavefunctions" (AX) schemes:

$$\begin{aligned}
\langle \Psi^J_{ia} | \hat{\mathcal{O}} | \Psi^I_{jb} \rangle_B &= - Tr_o(\boldsymbol{Y}_J^\dagger \mathcal{O}_o \boldsymbol{Y}_I) + Tr_v(\boldsymbol{X}_J \mathcal{O}_v \boldsymbol{X}_I^\dagger) - Tr_o(\boldsymbol{X}_I^\dagger \mathcal{O}_o \boldsymbol{X}_J) + Tr_v(\boldsymbol{Y}_I \mathcal{O}_v \boldsymbol{Y}_J^\dagger) \\
\langle \Psi^J_{ia} | \hat{\mathcal{O}} | \Psi^I_{jb} \rangle_{AX} &= \sum_{ia} \sum_{jb} c^{J\dagger}_{ia} \, c^I_{jb} \langle \tilde{\Psi}^J_{ia} | \hat{\mathcal{O}} | \tilde{\Psi}^I_{jb} \rangle \\
&= \left[Tr_v(\boldsymbol{X}_\beta \mathcal{O}_v \boldsymbol{X}_I^\dagger) + Tr_v(\boldsymbol{Y}_\beta \mathcal{O}_v \boldsymbol{X}_I^\dagger) + Tr_v(\boldsymbol{X}_\beta \mathcal{O}_v \boldsymbol{Y}_I^\dagger) + Tr_v(\boldsymbol{Y}_\beta \mathcal{O}_v \boldsymbol{Y}_I^\dagger) \right] \\
&\quad - \left[Tr_o(\boldsymbol{X}_I^\dagger \mathcal{O}_o \boldsymbol{X}_J) + Tr_o(\boldsymbol{X}_I^\dagger \mathcal{O}_o \boldsymbol{Y}_J) + Tr_o(\boldsymbol{Y}_I^\dagger \mathcal{O}_o \boldsymbol{X}_J) + Tr_o(\boldsymbol{Y}_I^\dagger \mathcal{O}_o \boldsymbol{Y}_J) \right] .
\end{aligned}$$

The second solution is more symmetric with respect to the *ph* and *hp* transitions than the one obtained from the bosonization (AX contains terms of the form $\boldsymbol{X}_I \mathcal{O} \boldsymbol{Y}_J$).

In "TDA" ($\mathbb{B} = 0$) the two solutions coincide.

Nonadiabatic couplings between excited states

The (AX) representation of the matrix elements $\langle \Psi_{ia}^{J} | \hat{\mathcal{O}} | \Psi_{jb}^{I} \rangle$ is used to compute nonadiabatic coupling vectors between excited states along nonadiabatic trajectories. [5]

$$\langle \Psi_{ia}^{J} | \nabla_R \hat{\mathcal{H}} | \Psi_{jb}^{I} \rangle = \sum_{ab} (X_J^\dagger X_I + X_J^\dagger Y_I + Y_J^\dagger X_I + Y_J^\dagger Y_I)_{ab} \langle \phi_b | \nabla_R \hat{\mathcal{H}} | \phi_a \rangle$$
$$- \sum_{ij} (X_I X_J^\dagger + Y_I X_J^\dagger + X_I Y_J^\dagger + Y_I Y_J^\dagger)_{ji} \langle \phi_i | \nabla_R \hat{\mathcal{H}} | \phi_j \rangle \, .$$

The numerical evaluation of the matrix elements $\langle \phi_b | \nabla_R \hat{\mathcal{H}} | \phi_a \rangle$ is done as in the case of couplings with the ground state.

---

[5] I.T., E. Tapavicza, U. Rothlisberger, *J. Chem. Phys.* **130**, 124107 (2009); I. T, B.F.E. Curchod, A. Laktionov, and U. Rothlisberger, *J. Chem. Phys.*, **133**, 194104 (2010).

Nonadiabatic couplings - examples

As always, the quality of the nonadiabatic couplings will depend on the *xc*-functional used

$$\mathbf{d}_{kj}[\{\phi_\cdot\}] = \langle \tilde{\Phi}_k(\mathbf{R}) | \nabla_{\mathbf{R}} | \tilde{\Phi}_j(\mathbf{R}) \rangle$$

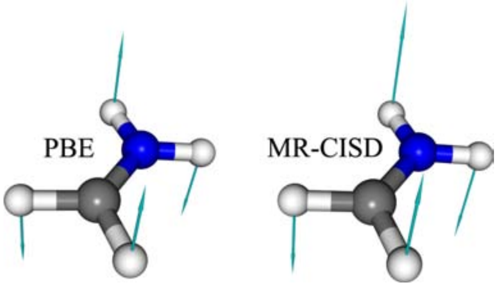

Protonated formaldimine: nonadiabatic coupling vectors $\mathbf{d}_{01}$ with LR-TDDFT/TDA.

Nonadiabatic couplings - examples

As always, the quality of the nonadiabatic couplings will depend on the *xc*-functional used

$$\mathbf{d}_{kj}[\{\phi_\cdot\}] = \langle\tilde{\Phi}_k(\mathbf{R})|\nabla_{\mathbf{R}}|\tilde{\Phi}_j(\mathbf{R})\rangle$$

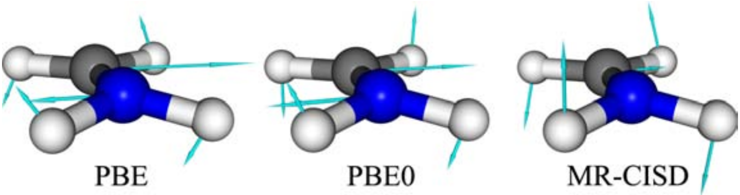

Protonated formaldimine: nonadiabatic coupling vectors $\mathbf{d}_{12}$ with LR-TDDFT/TDA.

Radiation damage in DNA

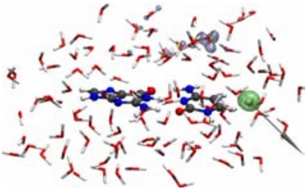

Photostability of proteins

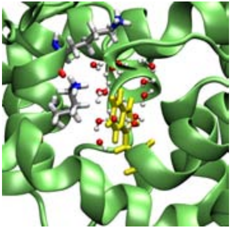

Protein/DNA interaction

NACV in design of new dyes

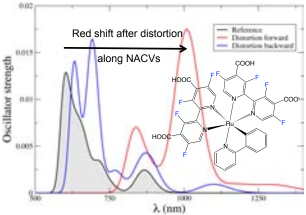

Ultrafast spectroscopy

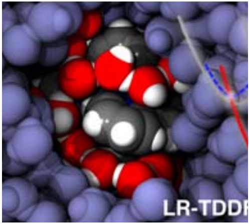

el.-ph. coupl. in graphene

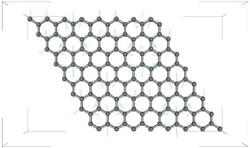

Electronic and vibration spectra of graphene

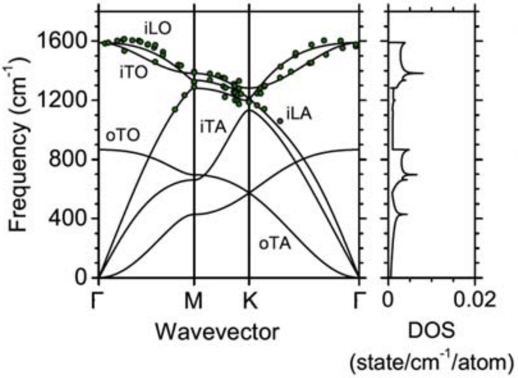

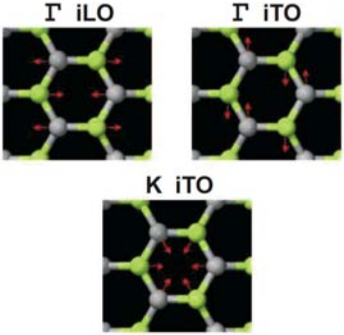

Electronic and vibration spectra of graphene

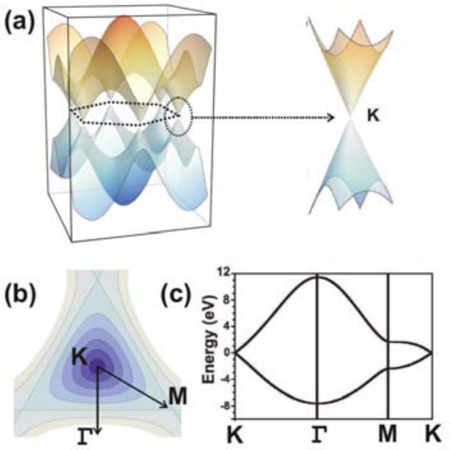

Calculation of the deformation potential

The key quantity in the calculation of the electron-phonon coupling is the ‘squared’ *deformation potential* [F. Mauri *et al.* (*PRB*, **78**, 081406(R), 2008)]

At Γ:

$$\langle D^2_\Gamma \rangle = \sum_{ij}^{\pi\pi^*} |\langle \mathbf{K}, j | \Delta V_{\Gamma \mathbf{E_{2g}}} | \mathbf{K}, i \rangle|^2 / 4$$

i, j: sum over the 2-times degenerate π-bands at **K**,

and at K:

$$\langle D^2_{\mathbf{K}} \rangle^{\pi\pi^*}_{\mathbf{k}} = |\langle 2\mathbf{K} + \mathbf{k}, \pi^* | \Delta V_{\mathbf{K} A'_1} | \mathbf{K} + \mathbf{k}, \pi \rangle|^2 / 2$$

$\langle \mathbf{K}, j | \Delta V_{\Gamma \mathbf{E_{2g}}} | \mathbf{K}, i \rangle$ is the deformation potential, which can be computed as the directional derivative along the E_{2g} mode

$$\nabla_{\mathbf{R}} H \cdot \delta \mathbf{R}_{\Gamma_{\mathbf{E_{2g}}}} \ .$$

Numerical calculation

The 'squared' distortion potentials are usually computed as a limit procedure

$$\langle D_{\mathsf{K}}^2 \rangle = \lim_{d\to 0} \frac{1}{8}\left(\frac{\Delta E_{\mathsf{K}}}{d}\right)^2$$

$$\langle D_{\Gamma}^2 \rangle = \lim_{d\to 0} \frac{1}{16}\left(\frac{\Delta E_{\Gamma}}{d}\right)^2$$

where $\Delta E_{\mathbf{X}} = \varepsilon_{\mathbf{X},\pi} - \varepsilon_{\mathbf{X},\pi^*}$, with $\mathbf{X} = \mathbf{K}, \Gamma$.

We compute the nonadiabatic couplings as product $\nabla_{\mathbf{R}} H \cdot \mathbf{R}_{\mathbf{X}}$ along a phonon mode $\mathbf{X}$

$$\mathcal{M} = -\frac{i}{\sqrt{N}} \sum_{\alpha} \sum_{\mathbf{k}\in\mathsf{FBZ}} \sum_{\lambda} \frac{l'_{\mathbf{k}\lambda}}{\sqrt{2}} \varepsilon_{\mathbf{k}\lambda} e^{i\mathbf{k}\cdot\mathbf{R}_{\alpha}^{\mathbf{0}}} \cdot \nabla_{\alpha} V(\mathbf{r} - \mathbf{R}_{\alpha}^{0})$$

Graphene supercells

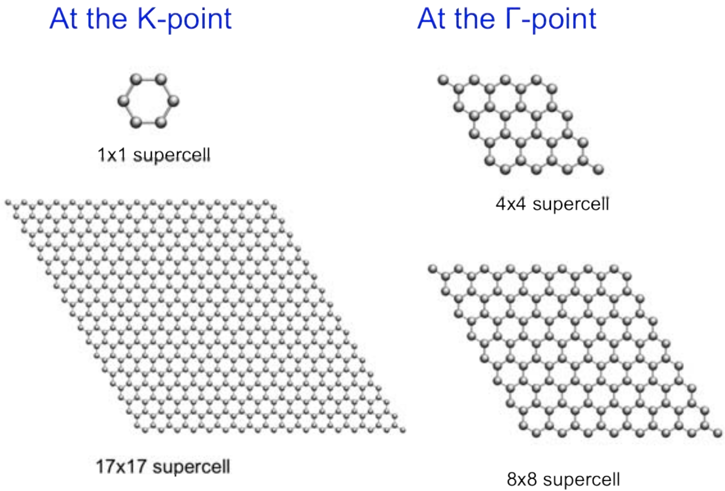

High energy vibrations at the K-point (A_1')

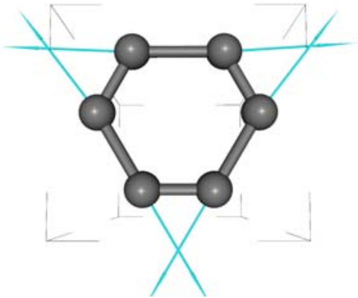

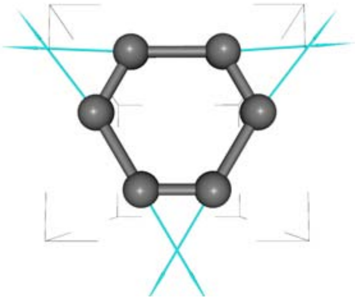

el-ph coupling in graphene from $\nabla_{\mathbf{R}} H \cdot \delta\mathbf{R}$

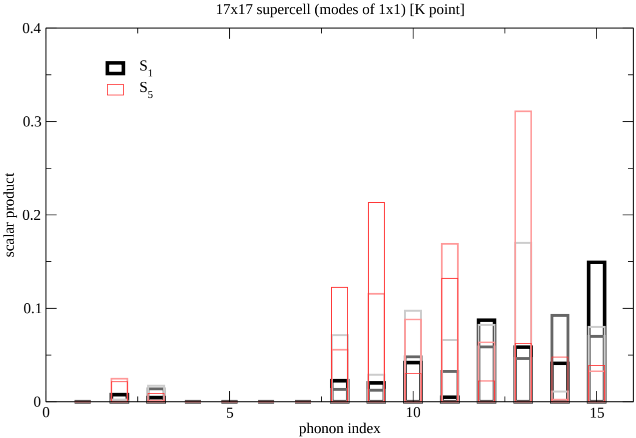

High energy vibrations at the Γ-point (E_{2g})

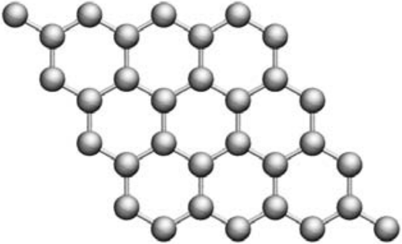

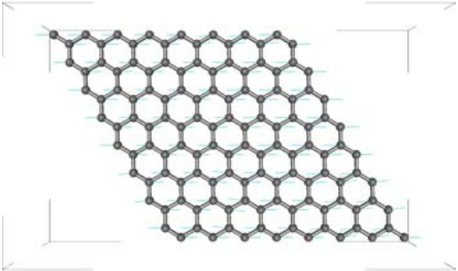

el-ph coupling in graphene from $\nabla_{\mathbf{R}} H \cdot \delta \mathbf{R}$

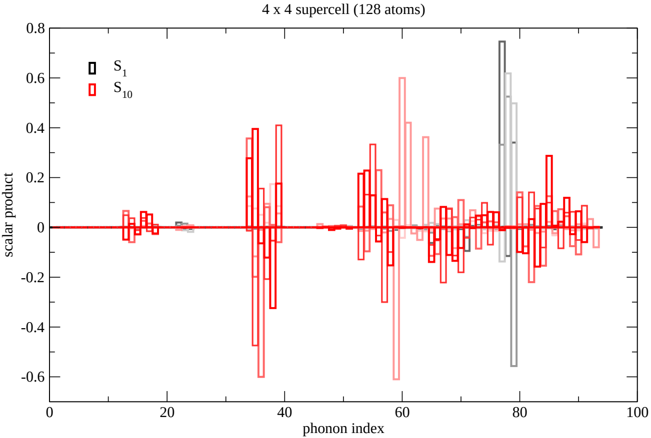

el-ph coupling in graphene from $\nabla_{\mathbf{R}} H \cdot \delta \mathbf{R}$

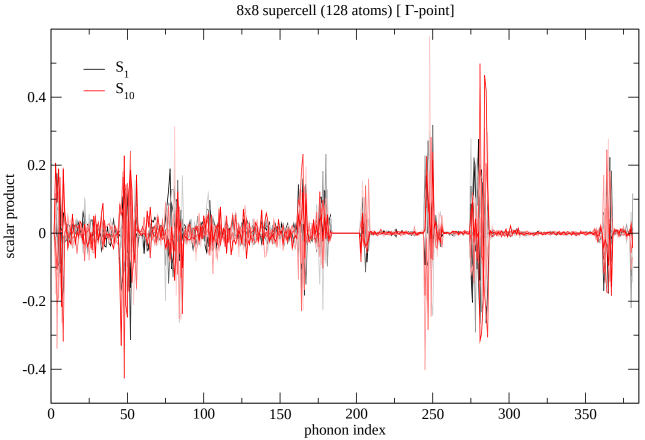

el-ph coupling in graphene from $\nabla_{\mathbf{R}} H \cdot \delta\mathbf{R}$

Mode at 1430 cm^{-1}

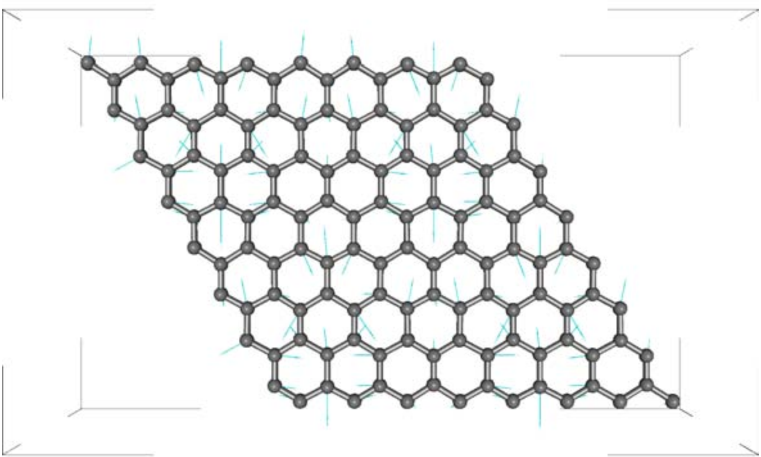

Acknowledgments

LCBC laboratory (EPFL)

- Ursula Roethlisberger
- Basile Curchod
- Andrey Laktionov

Implementations & documentation

CPMD	TDDFT/TSH (QM/MM + external EM field) available free of charge (for academics) from www.cpmd.org

Turbomol	Version by Vlasta Bonacic-Koutecky
Turbomol	Implementation in the group of F. Furche (by Enrico Tapavicza). Soon available in the official release of the code.
CP2K	Hopefully in the near future.
PetaChem	Collaboration with Todd Martinez

Thank you for your attention

QM/MM coupling with the excited electron density

The interaction energy between the QM and the MM is given by

$$E_{QM/MM} = \sum_{\gamma} q_{\gamma} \int v_{sC}(|\boldsymbol{R}_{\gamma} - \boldsymbol{r}|)\rho_0(\boldsymbol{r})d\boldsymbol{r} + \sum_{\gamma'\gamma} \frac{Z_{\gamma'} q_{\gamma}}{|\boldsymbol{R}_{\gamma'} - \boldsymbol{R}_{\gamma}|}$$
$$+ \frac{1}{2}\sum_{\gamma'}\sum_{\gamma} 4\epsilon_{\gamma'\gamma}\left[\left(\frac{\sigma_{\gamma'\gamma}}{|\boldsymbol{R}_{\gamma} - \boldsymbol{R}_{\gamma'}|}\right)^{12} - \left(\frac{\sigma_{\gamma'\gamma}}{|\boldsymbol{R}_{\gamma} - \boldsymbol{R}_{\gamma'}|}\right)^{6}\right]$$

In LR-TDDFT we use the LR density $\rho_I(\boldsymbol{r}) = \rho_0(\boldsymbol{r}) + \delta\rho_I(\boldsymbol{r})$

- In Casida's formalism: $\delta\rho_I(\boldsymbol{r}) = \sum_{pq} \Delta P^I_{pq} \xi^*_p(\boldsymbol{r})\xi_q(\boldsymbol{r})$ with $\Delta P^I_{pq} = -f_p f_q \left(\sum_a X^{I\dagger}_{pa} X^I_{qa} + \sum_a Y^{I\dagger}_{qa} Y^I_{pa}\right) + \tilde{f}_p \tilde{f}_q \left(\sum_i X^{I\dagger}_{iq} X^I_{ip} + \sum_i Y^{I\dagger}_{ip} Y^I_{iq}\right)$
- In the Sternheimer formalism

$$\delta\rho_I(\boldsymbol{r}) = \sum_i \phi_i(\boldsymbol{r})(\phi^{\{\pm\}}_{I,i})^*(\boldsymbol{r}) + \phi^{\{\pm\}}_{I,i}(\boldsymbol{r})\phi^*_i(\boldsymbol{r})$$

[Ref: IT, B. Curchod, U. Rothlisberger, *Chem.Phys.*, **391**, 101 (2011)]

Radiation damage in DNA

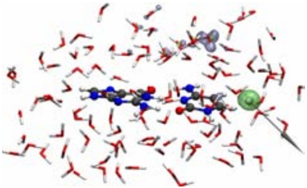

Photostability of proteins

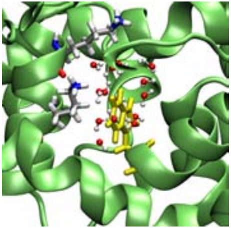

Protein/DNA interaction

NACV in design of new dyes

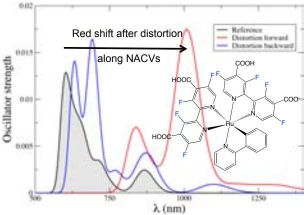

Ultrafast spectroscopy

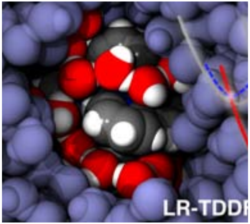

Excited states vibr. dynamics

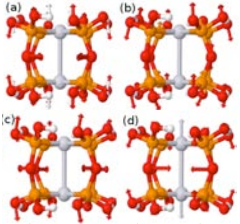

Collaboration: T. Penfold and M. Chergui

Ruthenium(II) tris-bipyridine ($[Ru(bpy)_3)]^{2+}$)

The "hydrogen atom" of all metal-to-ligand charge transfer processes (MLCT).

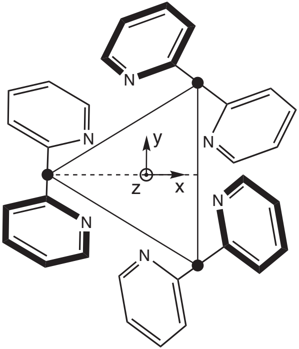

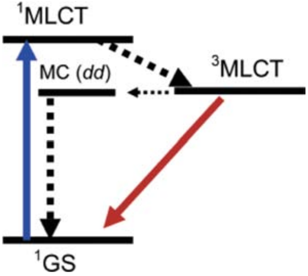

$[\mathrm{Ru(bpy)_3)}]^{2+}$: photophysics - experiments

Experiments available for Iron(II)-tris(bipyridine)
Ch. Bressler et al., *Science*, **323**, p489 (2009).

$<$ 100 fs $^{\mathbf{1}}$MLCT → $^{\mathbf{3}}$MLCT conversion

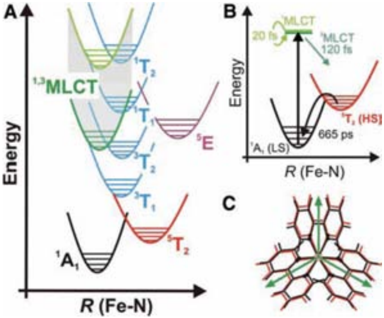

Kinetics of the 4-steps process
$^{\mathbf{1}}\mathrm{A}_{\mathbf{1}} \rightarrow {}^{\mathbf{1}}$ MLCT → $^{\mathbf{3}}$ MLCT → $^{\mathbf{5}}$T

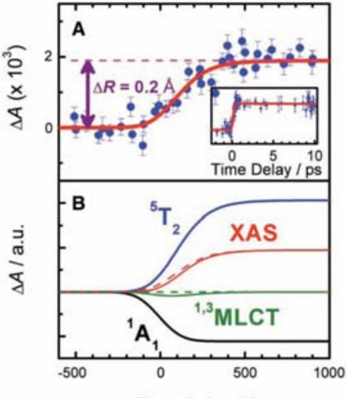

$[Ru(bpy)_3)]^{2+}$: photophysics - calculations

Nonadiabatic dynamics of $[Ru(bpy)_3)]^{2+}$ (DFT/TDFT) in solution (MM water)

GS	AIMD equilibration at 300 K in the GS [M.E. Moret, I.T., U. Rothlisberger, JPC B 2009, 113, 7737-7744]
Ex	vertical excitation $S_0 \rightarrow S_n$ singlet MLCT
S	on-the-fly TDDFT/MM TSH and crossings with the triplets [IT, B.F.E. Curchod, U. Rothlisberger, *accepted in the Chem.Phys.* (Special issue on TDDFT), 2011]
T	AIMD adiabatic of the ^{3}MLCT state [M.E. Moret, I.T., M. Chergui, U. Rothlisberger, Chem. Eur. J. 2010, 16, 5889 - 5894]

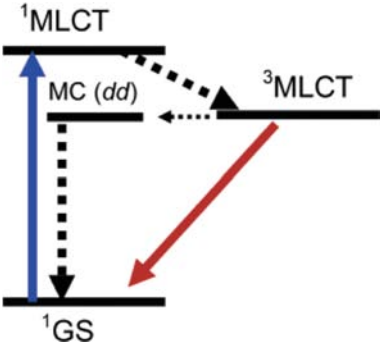

Solvation structure

The first solvation shell is well organized and plays a key role in the dynamics in the MLCT state (relazation times)

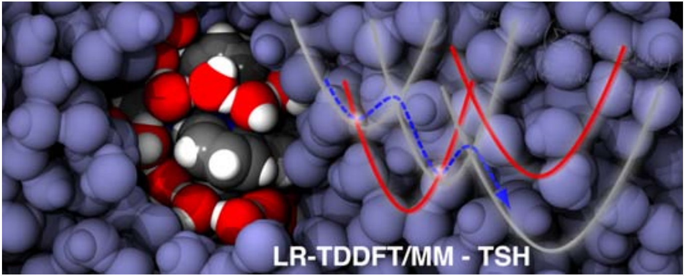

[M.E. Moret, I.T., U. Rothlisberger, JPC B 2009, 113, 7737-7744; IT, B.F.E. Curchod, U. Rothlisberger, *accepted in the Chem.Phys.* (Special issue on TDDFT), 2011]

$[Ru(bpy)_3)]^{2+}$: photophysics - dynamics on S_n

Two LR-TDDFT/MM TSH trajectories started in S_n state. At the crossings with the triplet SOC are computed. The ultrafast relaxation time for the ^{1}MLCT-^{3}MLCT transition is in agreement with experiments $(50 - 100fs)$

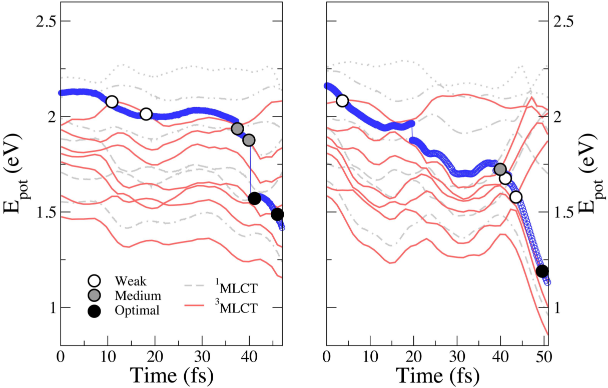

[IT, B.F.E. Curchod, U. Rothlisberger, *accepted in the Chem.Phys.* (Special issue on TDDFT), 2011]

$[\mathrm{Ru(bpy)_3)}]^{2+}$: Fast relaxation within the first solvation shell

The ultrafast rotation (libration) of the under-coordinated water molecule in the first solvation shell of the dye is responsible for the stabilization of the excited electron in the MLCT complex.

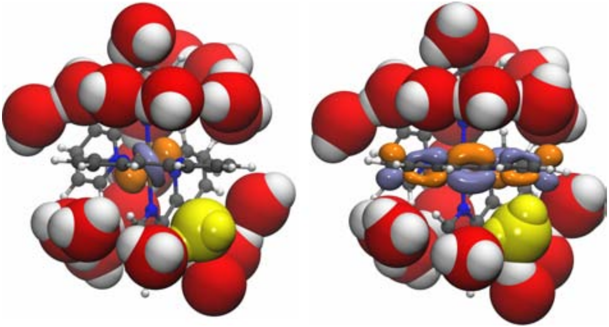

[IT, B.F.E. Curchod, U. Rothlisberger, *accepted in the Chem.Phys.* (Special issue on TDDFT), 2011]

$[Ru(bpy)_3)]^{2+}$: photophysics - dynamics in T_1

Excited electron localized on one or (mainly) two ligands (stabilization mediated by the solvent)

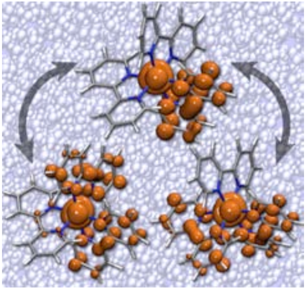

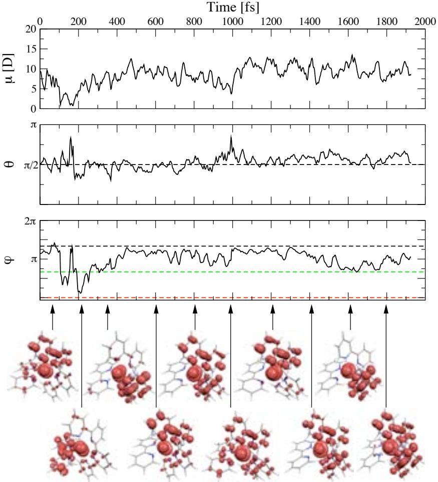

[M.E. Moret, I.T., M. Chergui, U. Rothlisberger, Chem. Eur. J. 2010, 16, 5889 - 5894]